Transportation dynamics on networks of mobile agents

Han-Xin Yang,[1] Wen-Xu Wang,[2] Yan-Bo Xie,[1] Ying-Cheng Lai,[2,3] and Bing-Hong Wang[1,4]

[1]*Department of Modern Physics, University of Science and Technology of China, Hefei 230026, China*

[2]*School of Electrical, Computer and Energy Engineering, Arizona State University, Tempe, Arizona 85287, USA*

[3]*Department of Physics, Arizona State University, Tempe, Arizona 85287, USA*

[4]*Research Center for Complex System Science, University of Shanghai for Science and Technology and Shanghai Academy of System Science, Shanghai 200093, China*

(Received 15 June 2010; revised manuscript received 27 September 2010; published 11 January 2011)

Most existing works on transportation dynamics focus on networks of a fixed structure, but networks whose nodes are mobile have become widespread, such as cell-phone networks. We introduce a model to explore the basic physics of transportation on mobile networks. Of particular interest is the dependence of the throughput on the speed of agent movement and the communication range. Our computations reveal a hierarchical dependence for the former, while an algebraic power law is found between the throughput and the communication range with the exponent determined by the speed. We develop a physical theory based on the Fokker-Planck equation to explain these phenomena. Our findings provide insights into complex transportation dynamics arising commonly in natural and engineering systems.

DOI: 10.1103/PhysRevE.83.016102 PACS number(s): 89.75.Hc, 02.50.−r, 05.40.Fb, 89.40.−a

I. INTRODUCTION

Transportation processes are common in complex natural and engineering systems, examples of which include transmission of data packets over the Internet, public transportation systems, migration of carbon in biosystems, and virus propagation in social and ecosystems. In the past decade, transportation dynamics have been studied extensively in the framework of complex networks [1–10], where a phenomenon of main interest is the transition from free flow to traffic congestion. For example, it is of both basic and practical interest to understand the effect of the network structure and routing protocols on the emergence of congestion [11–19]. Despite these works, relatively little attention has been paid to the role of *individual mobility*. The purpose of this paper is to address how this mobility affects the emergence of congestion in transportation dynamics.

The issue of individual mobility has become increasingly fundamental due to the widespread use of ad hoc wireless communication networks. The issue is also important in other contexts such as the emergence of cooperation among individuals [20] and species coexistence in cyclic competing games [21]. Recently, some empirical data of human movements have been collected and analyzed [22,23]. From the standpoint of complex networks, when individuals (nodes, agents) are mobile, the edges in the network are no longer fixed, requiring different strategies to investigate the dynamics on such networks than those for networks with fixed topology. In this paper, we introduce an intuitive but physically reasonable model to deal with transportation dynamics on such mobile or nonstationary networks. In particular, we assume in our model that communication between two agents is possible only when their geographical distance is less than a predefined value, such as the case of wireless communication. Information packets are transmitted from their sources to destinations through this scheme. To be concrete, we assume the physical region of interest is a square in the plane, and we focus on how the communication radius and the agent moving speed affect the transportation dynamics with respect to of the emergence of congestion. Our main results are the following. First, we find that congestion can occur for small communication range, limited forwarding capability, and low mobile velocity of agents. Second, the transportation throughput exhibits a hierarchical structure with respect to the moving speed and there is in fact an algebraic power law between the throughput and the communication radius, where the power exponent tends to assume a smaller value for higher moving speed. To explain these phenomena in a quantitative manner, we develop a physical theory based on solutions to the Fokker-Planck equation under initial and boundary conditions that are specifically suited to the transportation dynamics on mobile-agent networks. Our results have direct applications in systems of tremendous technological importance [24–26].

In Sec. II, we describe our model of mobile agents in terms of the transportation rule and the network structure. In Sec. III, we present numerical results on the order parameter, the critical transition point, and the average hopping time. In Sec. IV, a physical theory is presented to explain the numerical results. A brief conclusion is presented in Sec. V.

II. TRANSPORTATION RULE AND NETWORK STRUCTURE OF MOBILE AGENTS

In our model, N agents move on a continuous, square-shaped cell of size L with periodic boundary conditions. Agents change their directions of motion, θ, as time evolves, but the moving speed v is the same for all agents. Initially, agents are randomly distributed on the cell. After each time step, the position and moving direction of an arbitrary agent i are updated according to

$$x_i(t+1) = x_i(t) + v\cos\theta_i(t), \tag{1}$$

$$y_i(t+1) = y_i(t) + v\sin\theta_i(t), \tag{2}$$

$$\theta_i(t) = \Psi_i, \tag{3}$$

where $x_i(t)$ and $y_i(t)$ are the coordinates of the agent at time t, and Ψ_i is an N-independent random variable uniformly

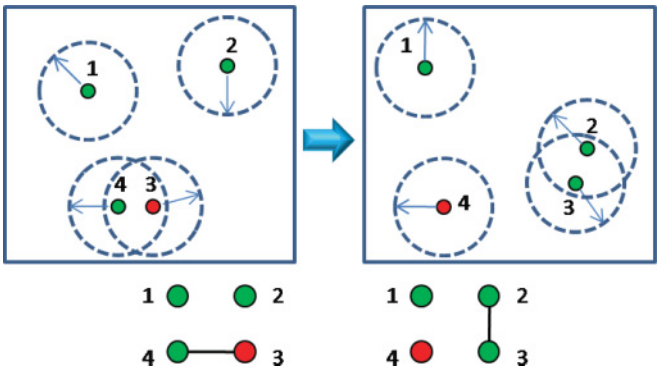

FIG. 1. (Color online) Schematic illustration of transportation process among mobile agents. The dashed circles denote the communication range, the arrows denote the moving directions, and each agent is specified by a number. Agents without data packets are in green (light gray) and agents holding data packets are in red (dark gray). The relevant communication networks are shown at the bottom.

distributed in the interval $[-\pi,\pi]$. Each agent has the same communication radius a. Two agents can communicate with each other if the distance between them is less than a. Variables a, v, and L share the same units of length. At each time step, there are R packets generated in the system with randomly chosen source and destination agents, and each agent can deliver at most C packets (we set $C = 1$ in this paper) toward its destination. To transport a packet, an agent performs a local search within a circle of radius a. If the packet's destination is found within the searched area, it is delivered directly to the destination and the packet is removed immediately. Otherwise, the packet is forwarded to a randomly chosen agent in the searched area. The queue length of each agent is assumed to be unlimited and the first-in-first-out principle holds for the queue. The transportation process is schematically illustrated in Fig. 1. In the left panel of Fig. 1, agents 3 and 4 can communicate with each other, where the former holds a packet. Agent 3 delivers the packet to agent 4 and then all agents move, as shown in the right panel of Fig. 1. After the movements, all agents randomly set new directions. There can be more than one agent in the communication range of any agent.

The communication network among the mobile agents can be extracted as follows. Every agent is regarded as a node of the network and a wireless link is established between two agents if their geographical distance is less than the communication radius a. Owing to the movement of agents, the network's structure evolves from time to time. The network evolution as a result of the local mobility of agents is analogous to a local rewiring process. As shown in Fig. 1, nodes 1 and 2 are disconnected while node 3 and node 4 are connected at time t. At time $t + 1$, nodes 1 and 2 depart from each other and become disconnected while nodes 3 and 4 approach each other and establish a communication link. Note that the mobile process does not hold the same number of links at different time, which is different from the standard rewiring process where the number of links is usually fixed.

We define an agent's degree at a specific time step as the number of links at that moment. Figure 2 shows that the

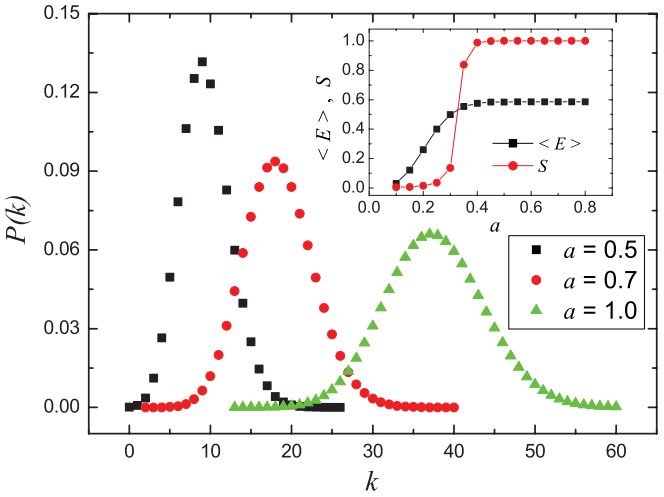

FIG. 2. (Color online) The fraction of nodes $P(k)$ as a function of degree k for different communication radius a. The inset shows the relative size S of the largest connected component and the clustering coefficient $\langle E\rangle$ as a function of communication radius a. The number of agents is 1200, the size of the square region is $L = 10$, and the velocity v is 0.1. We have examined that the topological properties are independent of v.

networks of mobile agents exhibit the Poisson distribution in their degrees:

$$P(k) = \frac{e^{-\langle k\rangle}\langle k\rangle^k}{k!}, \tag{4}$$

where k is the degree, $P(k)$ is the fraction of nodes with degree k, and $\langle k\rangle$ is the average degree of the network. As shown in Fig. 2, the average degree $\langle k\rangle$ increases as the communication radius a increases, and the peak value of $P(k)$ decreases as a increases. We also investigate the relative size of the largest connected component and the clustering properties of the network in terms of the clustering coefficient. The relative size S of the largest connected component is defined as

$$S = \frac{S_1}{N}, \tag{5}$$

where S_1 and N are the sizes of the largest connected component and of the total network, respectively. The clustering coefficient E_i for node i is defined as the ratio between the number of edges e_i among the k_i neighbors of node i and its maximum possible value, $k_i(k_i - 1)/2$; that is,

$$E_i = \frac{2e_i}{k_i(k_i - 1)}. \tag{6}$$

The average clustering coefficient $\langle E\rangle$ is the average of E_i over all nodes in the network. The inset of Fig. 2 shows that S and $\langle E\rangle$ increase as the communication radius a increases. In particular, when the value of a exceeds a certain value (e.g., 0.4), high values of S and $\langle E\rangle$ are attained. We also note that the motion speed does not influence the statistical properties of the communication network at each time step but affects the information transmission among agents, which is presented below. In general, the communication networks associated with limited searching area and mobile behavior have a Poisson distribution of node degrees and dense clustering structures.

III. NUMERICAL RESULTS

To characterize the throughput of a network, we use the order parameter η introduced in Ref. [1]:

$$\eta(R) = \lim_{t\to\infty} \frac{C}{R} \frac{\langle \Delta N_p \rangle}{\Delta t}, \tag{7}$$

where $\Delta N_p = N_p(t + \Delta t) - N_p(t)$, $\langle\cdot\rangle$ indicates the average over a time window of width Δt, and $N_p(t)$ represents the total number of data packets in the whole network at time t. As the packet-generation rate R is increased through a critical value R_c, a transition occurs from free flow to congestion. For $R \leqslant R_c$, owing to the absence of congestion, there is a balance between the number of generated and that of removed packets so that $\langle \Delta N_p \rangle = 0$, leading to $\eta(R) = 0$. In contrast, for $R > R_c$, congestion occurs and packets accumulate at some agents, resulting in a positive value of $\eta(R)$. The traffic throughput of the system can thus be characterized by the critical value R_c, which is on average the largest number of generated packets that can be handled at each time step without congestion.

Figure 3(a) exemplifies the transition in the order parameter $\eta(R)$ from free flow to congestion state at some critical value R_c. We find that R_c depends on both the moving speed v and the communication radius a. Figure 3(b) shows the dependence of R_c on v for different values of a. We observe a hierarchical structure in the dependence. Specifically, when v is less or larger than some values, R_c remains unchanged at a low and a high value, respectively, regardless of the values of v. The transition between these two values in R_c is continuous. The hierarchical structure can in fact be predicted theoretically in a quantitative manner (to be described). Figure 4(a) shows the dependence of R_c on a for different values of v, which indicates an algebraic power law: $R_c \sim a^\beta$, where β is the power-law exponent. We find that the power law holds for a wide range of a and the exponent β is inversely correlated with v. For example, for $v = 0$, $\beta \approx 3.5$, but for large values of v, say $v = 5$, we have $\beta \approx 2$. When a reaches the size of the square cell, R_c is close to N as every agent always stays in the searching range of all others and almost all packets can arrive at their destinations in a single time step.

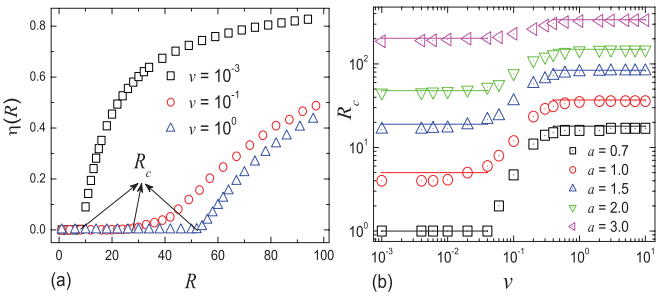

FIG. 3. (Color online) (a) Order parameter $\eta(R)$ vs R for different values of speed v and (b) dependence of the critical value R_c on v for different communication radius a. The number of agents is 1200 and the size of the square region is $L = 10$. In (a), $a = 1.2$ and $\eta(R)$ is obtained by averaging over 1×10^5 time steps after disregarding 2×10^4 initial steps as transients. The results in panels (a) and (b) are obtained by an ensemble average of 20 independent realizations. For each curve in panel (b), there are two fitting lines. The lower and upper lines for each value of a are the theoretical predictions from Eqs. (26) and (28), respectively.

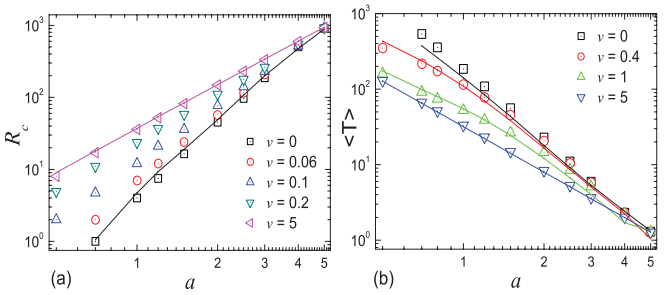

FIG. 4. (Color online) (a) Critical value R_c as a function of the communication radius a for different values of v. The lines are theoretical predictions from Eqs. (26) and (28). (b) Average hopping time $\langle T \rangle$ as a function of a for different values of v. The theoretical curves are obtained from Eqs. (20)–(23). For $v = 0.4$ and $v = 1$, $f = 1$ is used. Each data point is obtained by averaging over 20 independent realizations.

To develop a theory for the dependence of R_c on parameters a and v, we explore another important quantity, the average hopping time $\langle T \rangle$ in the free-flow state, where $\langle T \rangle$ is defined as the average number of hops for all data packets from their sources to destinations. Although the free-flow state is determined by $R < R_c$, where R_c is a function of the interaction radius a, moving velocity v, and delivering capacity C, we can simply set C to be infinity to satisfy the free-flow condition, regardless of the values of a, v, and R. Because of the absence of congestion, $\langle T \rangle$ in the free-flow state is determined only by a and v. (Except for the computation for $\langle T \rangle$ in the free-flow state, C is always set to be 1 for other simulations.) As we will see, not only can $\langle T \rangle$ be calculated numerically, it is also amenable to theoretical analysis, providing key insights into the transportation dynamics. Representative numerical results for $\langle T \rangle$ are shown in Fig. 4(b). We see that, for large v, $\langle T \rangle$ scales with a as a^{-2} and, as both v and a are increased, $\langle T \rangle$ decreases.

IV. THEORY

We now present a physical theory to explain the power-law behaviors associated with $\langle T \rangle$ and then R_c. A starting point is to examine the limiting case of $v = 0$, where $\langle T \rangle$ can be estimated analytically. In particular, assume that a particle walks randomly on an infinite plane. There are many holes, each of radius a, on the plane. Holes form a phalanx and the distance between two nearby holes is L. The particle stops walking when it falls in a hole. The underlying Fokker-Planck equation is

$$\frac{\partial P(\mathbf{r},t)}{\partial t} = [A\nabla^2 + U(\mathbf{r})]P(\mathbf{r},t), \tag{8}$$

where $P(\mathbf{r},t)$ is the probability density function of a particle at location $\mathbf{r}$ at time t, A is the diffusion coefficient, $U(\mathbf{r})$ is the potential energy, $U(\mathbf{r}) = -\infty$ inside holes and $U(\mathbf{r}) = 0$ outside holes, and $P(\mathbf{r},t) = 0$ inside holes and $P(\mathbf{r},t) > 0$ outside holes. Making use of solutions to the eigenvalue problem,

$$[A\nabla^2 + U(\mathbf{r})]\Phi_n(\mathbf{r}) = -\lambda_n \Phi_n(\mathbf{r}), \tag{9}$$

where $\Phi_n(\mathbf{r})$ is the normalized eigenfunction and λ_n is the corresponding eigenvalue, we can expand $P(\mathbf{r},t)$ as

$$P(\mathbf{r},t) = \sum_{n=1}^{\infty} c_n e^{-\lambda_n t}\Phi_n(\mathbf{r}), \tag{10}$$

where $c_n = \int P(\mathbf{r},0)\Phi_n(\mathbf{r})d\mathbf{r}$ and the initial probability density $P(\mathbf{r},0)$ is distributed over a region of size a. The probability that a particle still walks at time t is

$$Q(t) = \int P(\mathbf{r},t)d\mathbf{r} = \sum_{n=1}^{\infty} c_n d_n e^{-\lambda_n t}, \tag{11}$$

where $d_n = \int \Phi_n(\mathbf{r})d\mathbf{r}$. Since the $n = 1$ term is dominant, we have

$$Q(t) \approx c_1 d_1 e^{-\lambda_1 t}, \tag{12}$$

which gives the average hopping time as

$$\langle T\rangle \approx \frac{1}{\lambda_1}. \tag{13}$$

Since

$$\Phi_1(x,y) = \Phi_1(x+L,y) = \Phi_1(x,y+L), \tag{14}$$

the infinite-plane problem can be transformed into a problem on torus:

$$\begin{gathered}\nabla^2\Phi_1(r) = -h^2\Phi_1(r), \quad \text{for} \quad a < r < b,\\ \Phi_1(r=a) = 0, \quad \Phi_1'(r=b) = 0,\end{gathered} \tag{15}$$

where $b = L/\sqrt{\pi}$ and

$$\Phi_1(r) = B_1 J_0(hr) + B_2 N_0(hr). \tag{16}$$

J_0 and N_0 are the first- and second-kind Bessel functions, respectively, and $B_2 = -B_1 J_0(ha)/N_0(ha)$. The quantity h can be obtained by

$$\frac{J_0'(hb)}{J_0(ha)} = \frac{N_0'(hb)}{N_0(ha)}. \tag{17}$$

Using

$$J_0(x) \approx 1 - \frac{x^2}{4} + \frac{x^4}{64}, \tag{18}$$

$$N_0(x) \approx \frac{2}{\pi}\left[\left(\ln\frac{x}{2} + 0.5772\right)\left(1 - \frac{x^2}{4} + \frac{x^4}{64}\right) + \frac{x^2}{4} - \frac{3x^4}{128}\right], \tag{19}$$

and combining Eqs. (9) and (15), we get $\lambda_1 = Ah^2$. For $\Delta t = 1$, $\langle(\Delta r)^2\rangle = a^2/2$, we have $A = \langle(\Delta r)^2\rangle/4 = a^2/8$ and $\lambda_1 = Ah^2 = a^2h^2/8$. Finally, we obtain $\langle T\rangle$ as

$$\langle T\rangle \approx \frac{1}{\lambda_1} = \frac{8}{a^2h^2}. \tag{20}$$

For $v > 0$, $P(\mathbf{r},t)$ becomes zero in the area where a hole moves and $Q(t)$ decays with time under two mechanisms: diffusion at rate λ_1 and motion of holes at rate λ_w. Thus, we have

$$\langle T\rangle \approx \frac{1}{f\lambda_1 + \lambda_w}, \tag{21}$$

where f is the weighting factor ($0 \leqslant f \leqslant 1$) that decreases as v increases. Specifically, $f = 1$ for small v and $f = 0$ for large v. The quantity λ_w is given by

$$\lambda_w = \frac{\int_a^{v_s+a} r\Phi_1(r)\arccos\left(\frac{r^2+v_s^2-a^2}{2rv_s}\right)dr}{\pi\int_a^b r\Phi_1(r)dr}, \tag{22a}$$

$$\lambda_w = \frac{\int_{v_s-a}^{v_s+a} r\Phi_1(r)\arccos\left(\frac{r^2+v_s^2-a^2}{2rv_s}\right)dr}{\pi\int_a^b r\Phi_1(r)dr}, \tag{22b}$$

$$\lambda_w = \frac{a^2}{b^2} = \frac{\pi a^2}{L^2}, \tag{22c}$$

where $v_s = \sqrt{\langle|\mathbf{v}_1 - \mathbf{v}_2|^2\rangle} = \sqrt{2}v$, Eq. (22a) is valid for $0 < v_s < 2a < b - a$ or $0 < v_s < b - a < 2a$, Eq. (22b) is valid for $2a < v_s < b - a$, and Eq. (22c) is valid for $v_s > b - a$. For large values of v, agents are approximately well mixed so that we can intuitively expect the average time $\langle T\rangle$ to be determined by the inverse of the ratio of the agent's searching area and the area of the cell:

$$\langle T\rangle \approx \frac{L^2}{\pi a^2}. \tag{23}$$

The validity of this equation is supported by the fact that the ratio of the two areas is equivalent to the ratio of the total number of agents to the number of agents within the searching area. The estimation of $\langle T\rangle$ for large v is consistent with the theoretical prediction from Eqs. (21) and (22c) by inserting $f = 0$. The theoretical prediction is in good agreement with simulation results, as shown in Fig. 4(b).

With the aid of Eqs. (20) and (23) for $\langle T\rangle$, we can derive a power law for R_c. In a free-flow state, the number of disposed packets is the same as that of generated packets Rt in a time interval t. For $v = 0$, the number of packets n_i passing through an agent is proportional to its degree. This yields

$$n_i = \frac{R\langle T\rangle t k_i}{\Sigma_j k_j} = \frac{R\langle T\rangle t k_i}{N\langle k\rangle}, \tag{24}$$

where k_i is the degree of i, the sum runs over all agents in the network, and $\langle k\rangle$ is the average degree of the network. During t steps, an agent can deliver at most $C_i t$ packets. To avoid congestion requires $n_i \leqslant C_i t$. If all agents have the same delivering capacity C, the transportation dynamics is dominated by the agent with the largest number of neighbors and the transition point R_c can be estimated by

$$\frac{R_c\langle T\rangle t k_{\max}}{N\langle k\rangle} = Ct, \tag{25}$$

where $k_{\max}$ is the largest degree of the network. Thus, for $v = 0$, we have

$$R_c = \frac{NC\langle k\rangle}{\langle T\rangle k_{\max}}, \tag{26}$$

where $\langle k\rangle = N\pi a^2/L^2$. Since the degree distribution is $P(k) = e^{-\langle k\rangle}\langle k\rangle^k/k!$, the quantity $k_{\max}$ can be estimated by

$$\frac{e^{-\langle k\rangle}\langle k\rangle^{k_{\max}}}{k_{\max}!} \simeq \frac{1}{N}. \tag{27}$$

Inserting $\langle T\rangle$, $\langle k\rangle$, and $k_{\max}$ into Eqs. (26), we can calculate R_c for low moving speed v.

For large v, Eq. (26) can also be applied but for $k_{\max} = \langle k \rangle$ and $\langle T \rangle = L^2/\pi a^2$. Hence, R_c for large v is given by

$$R_c = \frac{NC}{L^2}\pi a^2. \tag{28}$$

Equation (28) indicates that R_c scales with a^2, which is in good agreement with the simulation results shown in Fig. 4(a).

V. CONCLUSION

In conclusion, we have introduced a physical model to study the transportation dynamics on networks of mobile agents, where communication among agents is confined in a circular area of radius a and agents move with fixed speed v but in random directions. In general, the critical packet-generating rate R_c at which the transition in the transportation dynamics from free flow to congestion occurs depends on both a and v, and we have provided a theory to explain the dependence. Our results yield physical insights into the dynamics of technological systems such as ad hoc wireless communication networks. For example, the power laws for the network throughput uncovered in this paper can guide the design of better routing protocols for such communication networks. Our findings are relevant to the dynamics in complex systems consisting of mobile agents, which is different from many existing works where no such mobility is assumed.

ACKNOWLEDGMENTS

This work is funded by the National Basic Research Program of China (973 Program No. 2006CB705500), the National Important Research Project (study on emergency management for non-conventional happened thunderbolts, Grant No. 91024026), the National Natural Science Foundation of China (Grants No. 10975126 and No. 10635040), and the Specialized Research Fund for the Doctoral Program of Higher Education of China (Grant No. 20093402110032). W.X.W. and Y.C.L. are supported by AFOSR under Grant No. FA9550-10-1-0083 and by NSF under Grants No. BECS-1023101 and No. CDI-1026710.

[1] A. Arenas, A. Díaz-Guilera, and R. Guimerà, Phys. Rev. Lett. **86**, 3196 (2001).
[2] B. J. Kim, C. N. Yoon, S. K. Han, and H. Jeong, Phys. Rev. E **65**, 027103 (2002).
[3] Z. Toroczkai and K. E. Bassler, Nature (London) **428**, 716 (2004).
[4] B. Tadić, S. Thurner, and G. J. Rodgers, Phys. Rev. E **69**, 036102 (2004).
[5] M. A. de Menezes and A.-L. Barabási, Phys. Rev. Lett. **92**, 028701 (2004).
[6] K. Park, Y.-C. Lai, L. Zhao, and N. Ye, Phys. Rev. E **71**, 065105 (2005).
[7] B. K. Singh and N. Gupte, Phys. Rev. E **71**, 055103(R) (2005).
[8] V. Cholvi, V. Laderas, L. López, and A. Fernández, Phys. Rev. E **71**, 035103(R) (2005).
[9] B. Danila, Y. Yu, J. A. Marsh, and K. E. Bassler, Phys. Rev. E **74**, 046106 (2006).
[10] G. Li, S. D. S. Reis, A. A. Moreira, S. Havlin, H. E. Stanley, and J. S. Andrade Jr., Phys. Rev. Lett. **104**, 018701 (2010).
[11] L. Zhao, Y.-C. Lai, K. Park, and N. Ye, Phys. Rev. E **71**, 026125 (2005).
[12] W.-X. Wang, B.-H. Wang, C.-Y. Yin, Y.-B. Xie, and T. Zhou, Phys. Rev. E **73**, 026111 (2006); W.-X. Wang, C.-Y. Yin, G. Yan, and B.-H. Wang, *ibid.* **74**, 016101 (2006).
[13] H. Zhang, Z. Liu, M. Tang, and P. M. Hui, Phys. Lett. A **364**, 177 (2007).
[14] X. Gong, L. Kun, and C.-H. Lai, Europhys. Lett. **83**, 28001 (2008).
[15] H.-X. Yang, W.-X. Wang, Z.-X. Wu, and B.-H. Wang, Phys. A **387**, 6857 (2008).
[16] M. Tang, Z. Liu, X. Liang, and P. M. Hui, Phys. Rev. E **80**, 026114 (2009).
[17] X. Ling, M.-B. Hu, R. Jiang, R. Wang, X.-B. Cao, and Q.-S. Wu, Phys. Rev. E **80**, 066110 (2009).
[18] B. Tadić and M. Mitrović, Eur. Phys. J. B **71**, 631 (2009).
[19] Y.-H. Xue, J. Wang, L. Li, D. He, and B. Hu, Phys. Rev. E **81**, 037101 (2010).
[20] D. Helbing and W. Yu, Proc. Natl. Acad. Sci. U. S. A. **106**, 3680 (2009).
[21] T. Reichenbach, M. Mobilia, and E. Frey, Nature (London) **448**, 1046 (2007).
[22] L. Hufnagel, D. Brockmann, and T. Geisel, Nature (London) **439**, 462 (2006).
[23] M. C. Gonzáles, C. A. Hidalgo, and A. L. Barabási, Nature (London) **453**, 779 (2008).
[24] L. Wang, C.-P. Zhu, and Z.-M. Gu, Phys. Rev. E **78**, 066107 (2008).
[25] E. M. Royer and C.-K. Toh, IEEE Person. Commun. **6**, 46 (1999).
[26] T. Camp, J. Boleng, and V. Davies, Wireless Commun. Mobile Comput. **2**, 483 (2002).